Flow Regimes in Centrifugal Partition Chromatography

M. J. van Buel, F. E. D. van Halsema, L. A. M. van der Wielen, and K. Ch. A. M. Luyben
Kluyver Inst. for Biotechnology, Delft University of Technology, Julianalaan 67, 2628 BC Delft, The Netherlands

Modeling pressure drop, stationary-phase holdup and separation efficiency in centrifugal partition chromatography (CPC) are hampered by restricted knowledge concerning the flow behavior of the liquid-liquid two-phase system. A transparent column (type CPC-LLN) was constructed to determine the flow behavior as a function of the flow rate, rotational frequency and the properties of the two-phase system. Two main types of flow regimes, droplets and (broken) jets, are observed although the spraying regime hardly occurred. Droplets occur at low flow rates and low rotational frequencies. The droplet regime changes into the (broken) jet regime when either the flow rate or the rotational frequency increases above a critical value. This critical value is described reliably by a dimensionless number correlation. A flow chart showing the type of flow regime as a function of the Weber number and the centrifugal force enables rational fine-tuning of operating conditions for given two-phase systems and equipment.

Introduction

Centrifugal partition chromatography (CPC) is a novel chromatographic technique in which the separation mechanism is based on the difference in distribution of components over two immiscible liquid phases. Figure 1 shows a CPC column that is placed in a rotor. The column consists of cartridges, in which channels are engraved that are connected by narrow ducts. The stationary phase stays in the channels due to the centrifugal force and the special column geometry. Different components introduced in the mobile phase as a mixture distribute differently over the two phases and consequently leave the column separated. A cartridge consists generally of 400 or more channel–duct combinations. Reported working volumes of CPC columns range from 125 mL to 30 L. Different cartridge and channel geometries are available (Foucault, 1995).

Foucault et al. (1994) introduced the "Stokes model," which describes the flow of the mobile phase in a channel as droplets with an average radius, corresponding to "Stokes' law." The average radius is calculated from the average linear velocity of the mobile phase in a channel, which in turn is calculated from stationary-phase holdup experiments (Foucault et al., 1992). The Stokes model is used to explain the stationary-phase holdup of various two-phase systems with different properties, and to explain the influence of the rotational frequency on the efficiency (measured in terms of the number of theoretical plates) of a separation. The authors indicate that a direct visualization of the mobile-phase flow through the stationary phase would be very useful.

Armstrong et al. (1988) developed a mass-transfer model to describe the separation efficiency of CPC separations as a function of the flow rate of the mobile phase. They assume that the bulk of the mass transfer is occurring while the mobile phase is present as an emulsified band between the two phases. However, no visual evidence of the presence of such an emulsified band was presented.

Van Buel et al. (1995) presented photographs of the typical flow regimes occurring in the channels of a CPC-LLN column for the water/hexane two-phase system at various flow rates and rotational frequencies. The photographs show pictures of the droplet regime and the (broken) jet regime. The photographs may explain the discrepancy between the predicted and experimental pressure drop over a CPC column. It was shown that for relatively high rotational frequencies, part of the stationary phase is forced into the duct. This effectively decreases the stationary-phase height in a channel, and thereby the hydrostatic pressure drop over a CPC column.

The examples given earlier indicate the need for information on the type of flow regimes occurring in a CPC channel.

Correspondence concerning this article should be addressed to L. A. M. van der Wielen.

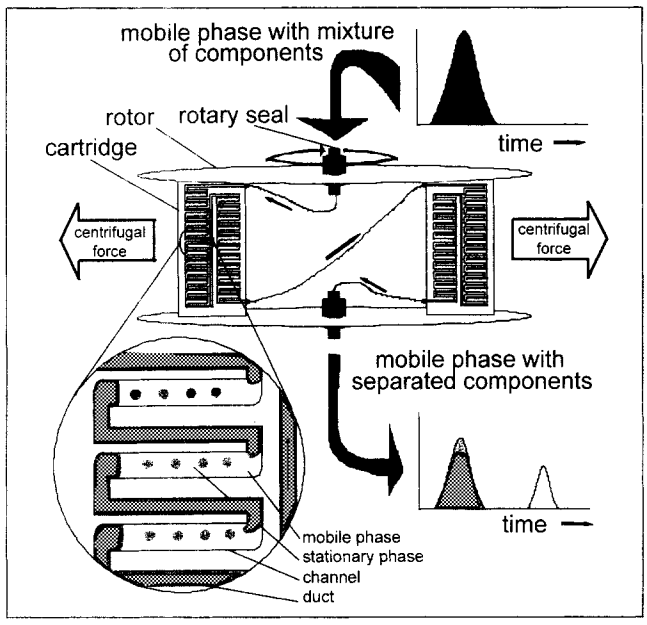

Figure 1. Centrifugal partition chromatograph.

In this article, the type of flow regime in a CPC channel is related to the operating conditions (flow rate and rotational frequency) and the properties of the two-phase system. A dimensionless correlation is presented for prediction of the critical values at which the transition between the droplet regime and the (broken) jet regime occurs.

Materials and Methods

Materials

1-Octanol (> 95%), *n*-butanol (> 99%), *n*-heptane (> 99%), *n*-hexane (> 99%), ethyl acetate (> 99%), and chloroform (> 99%) were purchased from J. T. Baker B.V., Deventer, Holland. Methanol (> 99.8) was purchased from Acros, Geel, Belgium. Water was demineralized. Several two-component two-phase systems were used. In addition, a three-component two-phase system was used at three different compositions: heptane/methanol/water-50/37.5/12.5 vol. % (HMW 12.5), heptane/methanol/water-50/25/25 vol. % (HMW 25), and heptane/methanol/water-50/12.5/37.5 vol. % (HMW 37.5). Table 1 gives an overview of the selected two-phase systems. The dye used in the visual experiments was nigrosin.

Transparent CPC-LLN cartridge

A transparent CPC cartridge and a rotor were constructed by the workshop of the Kluyver Laboratory for Biotechnology, Delft. The channel and duct dimensions and geometries are equal to those of the commercial CPC-LLN 250W cartridges (Van Buel et al., 1995). The channels and ducts are engraved in a 2-mm-thick Teflon plate. The Teflon plate was clamped between two plates of polycarbonate and fitted in a brass frame. Between the engraved Teflon plate and the polycarbonate plate, a Teflon sheet of 0.05 mm was tightened to ensure a leakage-free cartridge. The channel is 1.15 mm deep, 2.5 mm wide, and 12.6 mm long. The duct is 0.95 mm deep, 1 mm wide, and its total length is 14.6 mm. By using an optical system of two mirrors and a stroboscope, the images were "freezed" (see Figure 2). Three channel–duct combinations are visible in the mirror. The position of the mirror on the cartridge could be adjusted in height to observe different channels. The average distance between the channels visible in the mirror and the rotor axis (R) is 0.199 ± 0.001 m.

Table 1. Experimental Determined and Literature Values Found for the Interfacial Tensions of the Selected Two-Phase Systems at 293 K

Two-Phase System	Conc. of Nigrosin (g/L)	Interf. Tension Exp. (mN/m)	Interf. Tension Jufu et al. (1986) (mN/m)
n-Hexane/water	0	40.74 ± 0.22	49.75
	0.2	41.12 ± 0.39	
n-Heptane/water	0	45.86 ± 0.15	50.2
	0.19	44.97 ± 1.63	
n-Butanol/water	0	1.67 ± 0.00	1.8
	0.22	1.61 ± 0.01	
n-Octanol/water	0	8.24 ± 0.01	8.5
	0.06	8.08 ± 0.03	
Ethyl acetate/water	0	6.32 ± 0.03	6.8
	0.22	6.25 ± 0.02	
Chloroform/water	0	30.94 ± 0.04	31.6
	0.22	30.94 ± 0.04	
HMW 37.5	0	24.63 ± 0.1	—
HMW 25	0	13.86 ± 0.07	—
HMW 12.5	0	7.48 ± 0.09	—

Experimental procedure

The transparent CPC cartridge and the setup to perform the visual observations is shown in Figure 2. By adding the dye nigrosin to the mobile phase it is possible to distinguish between the stationary and the mobile phase. An experiment was started by rinsing the setup with acetone and subsequently filling the column with the stationary phase. After startup of the rotor, the mobile phase was pumped through the column. Photographs were taken using a Pentax Z-20 camera equipped with a 70–210-mm zoom lens and a 50-mm extension tube. All experiments were performed with an aqueous mobile phase, because the dye was soluble in water only. To determine the experimental conditions at which the droplet–jet transition occurs, the column was filled and a rotational frequency was set. Later, the flow rate was increased by increments of 0.1 mL/min. The droplet–jet transition was determined visually.

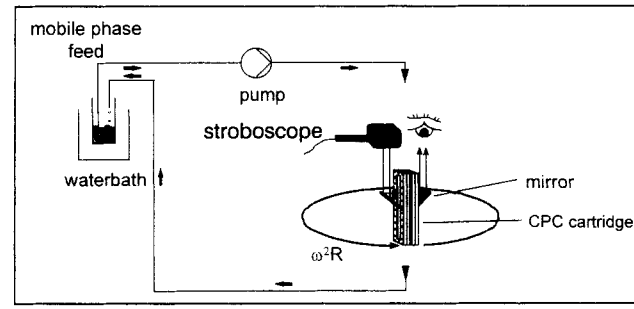

Figure 2. Experimental setup for the visual experiments.

Measurement of interfacial tension and phase density

The interfacial tensions of the water/organic two-phase systems were measured with a fully automated Lauda TVT1 drop-volume tensiometer. The principle of the drop-volume technique is to measure the volume (or weight) of a drop that has just detached from the tip of a capillary. The interfacial tension is calculated from this volume and the capillary diameter. The densities of the upper and lower phase of the two-phase systems were measured at 20°C with an oscillating-cell density meter (AP Paar density meter DMA 48).

Results and Discussion

Properties of the two-phase system

Table 1 gives the interfacial tension for the two-component two-phase systems with and without 0.21 ± 0.02 g nigrosin added to the mobile phase. The interfacial tension of the HMW two-phase systems were determined without dye. The nigrosin concentration given in Table 1 was equal to the concentration used during the visual CPC experiments. The influence of nigrosin on the interfacial tension is small (maximum 4% of *n*-butanol/water). Apart from the heptane/water two-phase system and the hexane/water two-phase system the measured interfacial tension agrees well with the values given by Jufu et al. (1986). The measured interfacial tension for the heptane/water two-phase system and the hexane/water two-phase system differ significantly, while the values given by Jufu et al. (1986) are almost equal. However, Scheele and Meister give a value of 36.2 N/m for the interfacial tension of the heptane/water two-phase system. The differences in interfacial tension measured by different authors might be caused by the presence of small amounts of surface-active components, effectively decreasing the interfacial tension.

Table 2 gives the densities and viscosities of the selected two-phase systems. The viscosities of the upper and lower phase of the heptane/water, hexane/water, and chloroform/water two-phase systems were considered equal to those of the pure liquids, since the mutual solubilities in these two-phase systems are small (Sørensen and Arlt, 1980). The viscosity of the upper (heptane) phase of the HMW two-phase systems is considered equal to the viscosity of pure heptane, since the solubilities of methanol and water in heptane are small at these compositions (Conway, 1989). The viscosity of the lower (water/methanol) phase of the HMW two-phase systems was calculated using the viscosity data of Weast (1980) for methanol/water mixtures. The viscosities of the upper and lower phases of the other two-phase systems were calculated using the method of Teja and Rice (1981).

Table 2. Densities and Viscosities of the Selected Two-Phase Systems at 293 K

Two-Phase System	Density Upper Phase (kg/m^3)	Density Lower Phase (kg/m^3)	Viscosity Upper Phase (mPa·s)	Viscosity Lower Phase (mPa·s)
n-Hexane/water	660	998	0.33	1.00
n-Heptane/water	684	986	0.42	1.00
n-Butanol/water	878	969	3.49	1.46
n-Octanol/water	832	998	8.1	1.00
Ethyl acetate/water	905	998	0.52	1.07
Chloroform/water*	1,001	1,487	1.0	0.58
HMW 37.5	680	964	0.42	1.77
HMW 25	680	924	0.42	1.68
HMW 12.5	680	865	0.42	1.15

*Water is the less dense phase!

Visual observations

The hydrodynamics of liquid breakup at an orifice under gravitational force is described and modeled by many people (Clift et al., 1978; Thornton, 1992). In general, at low flow rates individual drops are formed at the orifice. At increased flow rates the droplets form a jet that breaks up through axisymmetric amplification of surface perturbations. This is called varicose breakup. By increasing the flow rate, the jet length increases until a maximum jet length is reached. Above flow rates corresponding to this maximum jet length, the jet length decreases again, due to the growth of asymmetric disturbances. This mechanism is called sinuous breakup. The jet is then waving like a flag while lumps of liquid are breaking irregularly from the jet's tip. Increasing the flow rate further will reduce the jet length to zero. Small particles are formed immediately or at a short distance from the orifice; this is called the spray or atomization regime. The interfacial tension appears to be the most dominant property determining the type of flow regime. Therefore, the mass transfer from or to a droplet or jet (that influences the interfacial tension), or the presence of surface-active agents is expected to have a significant effect on the drop size, jet length, or jet diameter.

The conditions in a CPC channel are considerably different from the "ideal" conditions at which most of the flow regime characterization experiments under gravitational conditions were performed. First, instead of a gravitational force, the mobile phase is subjected to a centrifugal force that can exceed the gravitational force by a 1,000-fold. Second, the direction of the mobile-phase flow into the channel is perpendicular to the direction of the channel and the centrifugal force. Furthermore, the orifice is not circular but square, and the orifice is not perfectly "wetted" because part of the stationary phase is forced into the duct due to the centrifugal force (Van Buel et al., 1995). Finally, the size of the channel is limited with respect to the length and width. Instead of flowing into an "infinitely" large volume, the orifice is surrounded by channel walls and the mobile-phase flow is limited by the length and the width of the channel. For example, a jet that would break up under nonrestricted conditions, may reach the end of the channel before breakup, or may flow along the walls of the channel due to the limited width of the channel. The actual height of the stationary phase is determined by the stationary-phase holdup. Effects of mass transfer on the flow behavior were not taken into account during the present study.

Figure 3 shows photographs of the two flow regimes that were observed in the CPC channels under practical conditions: droplets and jets. The droplet regime is present at low rotational frequencies and low flow rates. The droplet regime transforms into the jet regime when the flow rate is increased above a critical value (for a given rotational frequency). The exact value of the critical flow rate depends on the properties of the two-phase system. The jet can either be continuous or breaking up in smaller droplets.

Figure 4 shows the flow characteristics of the droplet regime as a function of the flow rate and the rotational fre-

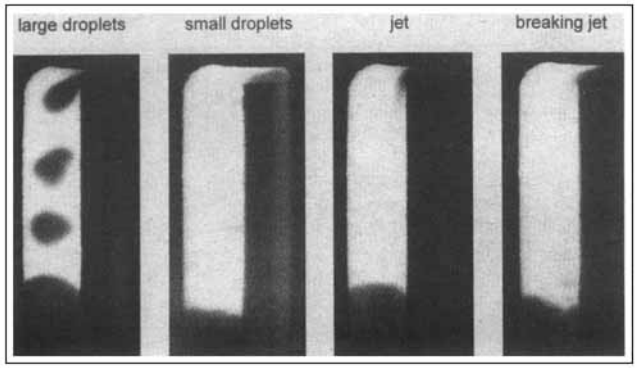

Figure 3. Various flow regimes in the CPC-LLN cartridge.

quency. At a low flow rate, a single droplet is observed. When the flow rate is increased more droplets appear with the same size and with an equal distance between them. When the flow rate is increased further, the droplets merge into an unbroken jet. When the rotational frequency is increased the droplets become smaller and eventually also change into an unbroken jet. The critical flow rate decreases with increasing rotational frequency. At relatively high rotational frequency (depending on the specific two-phase system that is used), when the droplets are very small and the transition between the droplet and the jet regime occurs at low flow rates, it is difficult to distinguish between a droplet or a jet regime.

The droplets that are formed have a diameter in the range 0.1–2.0 mm. Especially, the droplets larger than 1 mm in diameter are not spherical since the channel is only 1 mm deep. They move through the channels in a disk-like shape (see Figure 3, large droplets). Once a droplet is formed it does not break up. This is probably due to the relatively small size of the droplets.

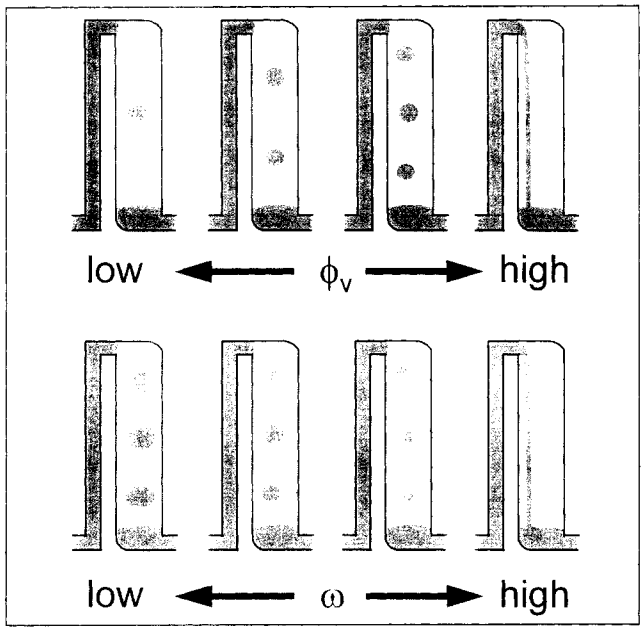

Figure 4. Influence of the flow rate and rotational frequency on the droplet flow behavior.

When the droplet regime has changed into the jet regime it is not possible to obtain the droplet regime again by simply decreasing the flow rate by 0.1 mL/min. The flow rate has to be decreased by 20–50% before the droplet regime appears again. When the flow rate is again increased from that point on, the droplet–jet transition occurs at the same critical flow rate. This means that it is possible to obtain both flow regimes in the flow-rate range around the critical flow rate (hysteresis).

The chloroform/water two-phase system is the only system from those tested, that shows a different behavior from the one described in Figure 4. At low flow rates the interface of the droplets is irregular, and the droplets flow through the stationary phase in clusters of droplets with unequal size (see Figure 5). When the flow rate is increased, the droplets become increasingly alike and move through the stationary phase at an equal distance from each other, as observed for the other two-phase systems. When the flow rate is increased, the string of droplets changes into a broken jet. For all other two-phase systems, the droplets always changed into an *un*broken jet. The droplets that are formed from the broken jet are smaller than the droplets that are formed directly at the orifice, which makes it possible to distinguish between the droplet and the broken jet regimes. The difference in droplet formation and transition behavior between the chloroform/water two-phase system and the other two-phase systems might be due to the large difference in density between the two phases of the chloroform/water two-phase system.

The jet regime has many appearances. The jet might be unbroken and flowing freely through the channel (Figure 6b) or along the wall (Figures 6a and 6c). The jet might also be broken (Figures 6d, 6e and 6f). The jet can break up in a single string of droplets or produce a spray of droplets (Figures 6g and 6h). At high rotational frequencies and high flow rates, the spray of droplets becomes so dense that it is difficult to distinguish individual droplets (Figure 6i). Furthermore, a large loss of stationary phase was observed when the column was run at spraying conditions (column bleeding).

Due to the limited dimensions of the channels, it is difficult to predict when a jet is unbroken, broken, or spraying as a function of the flow rate, rotational frequency, and the properties of the two-phase system. However, it is possible to give some general guidelines. First, the unbroken jet appears

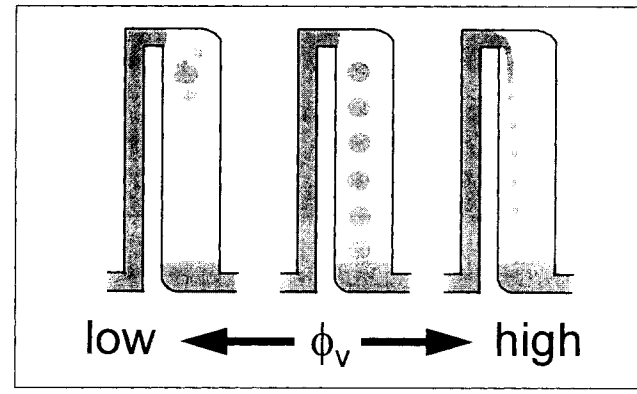

Figure 5. Influence of the flow rate and rotational frequency on the droplet flow behavior for the chloroform/water two-phase system.

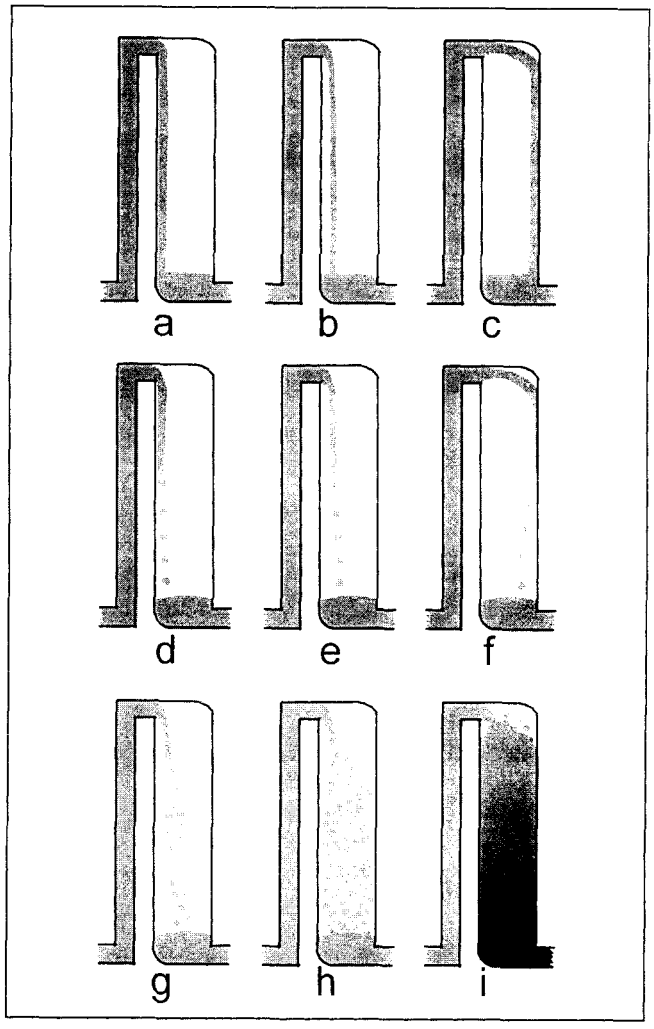

Figure 6. Various appearances of the jet regime.

when the droplet regime transforms into the jet regime. For the chloroform/water two-phase system no unbroken jet regime was detected, indicating that a large difference in density and therefore a large centrifugal force ($\Delta\rho\omega^2R$) causes breakup of the jet, where $\Delta\rho$ is the density difference between mobile and stationary phase (kg/m^3). The diameter of the jet increases at increasing flow rate. At low flow rates the jet tends to flow directly along the wall from the channel entrance (Figures 6a and 6d). At increased flow rates the jet flows through the channel or crosses the channel and flows along the wall at the opposite side from the channel entrance (Figures 6b, 6c, 6e, 6f). Jet spraying occurs at high rotational frequencies and high flow rates. The higher the flow rate and rotational frequency, the more dense the spray becomes (Figure 6g → 6h → 6i). Furthermore, spraying appears to start at lower rotational frequencies and flow rates for two-phase systems with a relatively low interfacial tension (e.g., *n*-butanol/water, HMW 12.5).

Apart from extreme experimental conditions at very high rotational frequencies and flow rates, no emulsion layer in the channels could be detected, as suggested by Armstrong et al. (1988). For example, the *n*-octanol/water two-phase system only shows the droplet and jet regime within the experimental conditions indicated by Armstrong et al. The centrifugal forces acting on the droplets that are formed directly at the channel entrance or from the breakup of a jet, collide with a high velocity with the mobile/stationary phase interface, causing the droplets to break up.

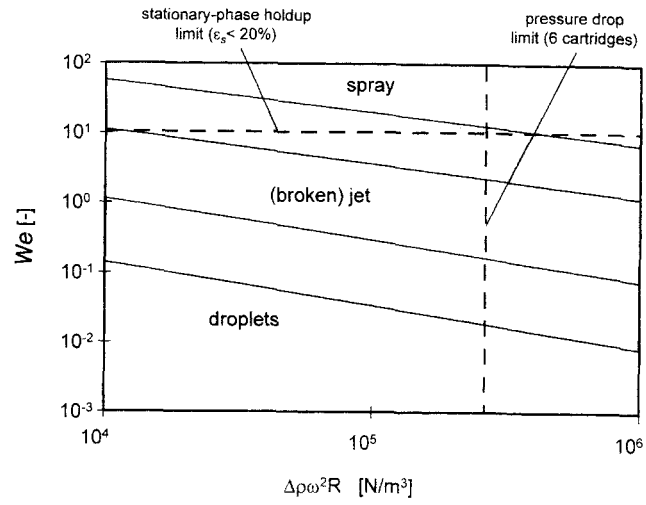

Figure 7. CPC-LLN cartridge.

Flow chart

To provide a more quantitative insight into the type of flow regime that occurs as a function of the experimental conditions and the properties of the two-phase system, a flow chart was constructed. Figure 7 shows a flow chart for the CPC-LLN cartridge as a function of the Weber number (*We*) and the centrifugal force ($\Delta\rho\omega^2R$). Figure 8 is based on 134 experimental points (experimental observations of the droplet (broken), jet, and spray regime for various two-phase systems and experimental conditions). The Weber number is the ratio of the inertia forces and the interfacial forces and is defined as:

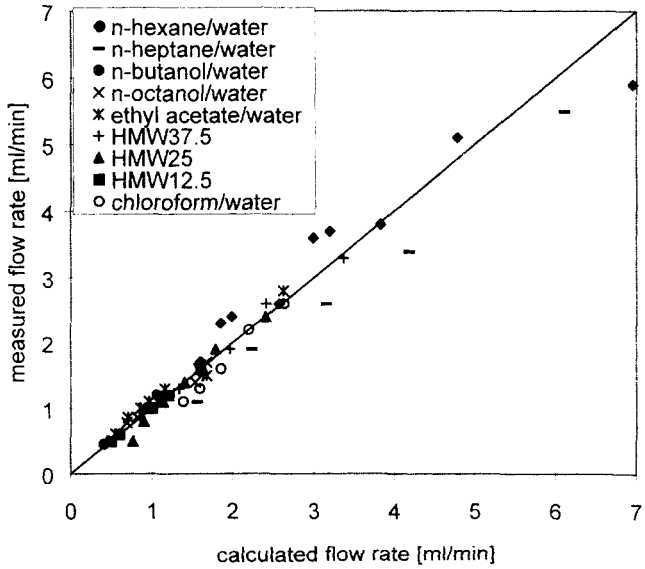

Figure 8. Parity plot of the critical flow rate.

$$We = \frac{\rho_s v^2 d_h}{\sigma}, \quad (1)$$

where ρ_s is the density of the stationary phase, v is the velocity at the channel entrance, d_h is the hydraulic diameter of the channel entrance, and σ is the interfacial tension. The hydraulic diameter for the CPC-LLN column is equal to 9.9×10^{-4} m. The flow-regime chart was constructed by determining the flow-regime transitions (droplet/jet, jet/broken jet, broken jet/spray) of five two-phase systems with a wide range of properties (*n*-heptane/water, *n*-butanol/water, ethyl acetate/water, *n*-octanol/water, and chloroform/water) as a function of the flow rate and the rotational frequency. Three flow regimes are distinguished: the droplet regime, at low Weber numbers and low centrifugal force; the spray regime, at high Weber number and high centrifugal force; and the (broken) jet regime. The region where two regimes occur (droplets/jet and (broken) jet/sprays) are indicated by the gray bands. Drawing a distinction between the jet regime and the broken-jet regime is difficult. The reason for this is probably that in principle every jet will break up if the channel is long enough. Still, Figure 7 gives an idea which flow regime can be expected for the CPC-LLN cartridge as a function of the properties of the two-phase system and the experimental conditions. It is anticipated, though not verified, that similar flow charts will hold for CPC equipment with different geometries.

Figure 7 also shows the pressure drop-limit and the phase-stability limit for the CPC-LLN cartridge (dashed lines). The maximum pressure drop over a CPC-LLN column is restricted by the rotary seals, which frequently show leakage at prolonged use at high operating pressures (> 60 bar). The total pressure drop over a CPC-LLN cartridge is mainly determined by the hydrostatic pressure drop (ΔP_{stat}; Van Buel et al., 1995):

$$\Delta P_{stat} = \Delta \rho \omega^2 R \frac{\epsilon_s V}{A_c}, \quad (2)$$

where ϵ_s is the stationary-phase holdup, V is the total column volume, and A_c is the cross-sectional area of the channel. The pressure-drop limit indicated in Figure 7 is therefore independent of the type of two-phase system; however, it depends on the total volume of the column. The pressure-drop limit indicated in Figure 7 is valid for a CPC-LLN column consisting of six cartridges (120 mL), which is the minimum volume reported in the literature for a separation.

The resolution of a CPC separation decreases with decreasing stationary-phase holdup (Foucault et al., 1994). The stationary-phase holdup for a given two-phase system as a function of the flow rate can be calculated using the holdup model of Foucault et al. (1994). The stationary-phase holdup is hardly a function of the rotational frequency (Foucault et al., 1994). The maximum stationary-phase holdup for the CPC-LLN cartridge is roughly 69%. The phase-stability limit indicated in Figure 7 is based on a stationary-phase holdup of 20%. Using the holdup model of Foucault et al. (1994), the flow rate at which the stationary phase drops below 20%, and the corresponding critical Weber number are calculated. This critical Weber number is 10–30, depending on the type of two-phase system.

Considering the limits to the Weber number (phase stability) and centrifugal force (pressure drop) indicated in Figure 7, it is clear that only two flow regimes are present in the channels of a CPC-LLN cartridge under practical conditions: the droplet regime and the (broken) jet regime. Therefore, it is important to get a more accurate prediction at which critical flow rate (for a given rotational frequency) the transition between the droplet and the jet regime occurs.

Prediction of the droplet–jet transitions

The prediction of the critical flow rate at which the transition between the droplet and the jet regime occurs (for a given rotational frequency) is based on a dimensionless-number correlation. The correlation was derived using dimensional analysis, assuming that the critical velocity (critical flow rate divided by the orifice cross-sectional surface) of the mobile phase at the channel entrance (v_{crit}) is a function of several variables:

$$v_{crit} = v_{crit}(\rho_s, \rho_m, \Delta \rho \omega^2 R, d_h, \sigma), \quad (3)$$

where ρ_m is the density of the mobile phase. The following dimensionless correlation was found:

$$We = aEo^b \left(\frac{\rho_s}{\rho_m}\right)^c, \quad (4)$$

where the Eötvos number ($E\ddot{o}$) is

$$E\ddot{o} = \frac{\Delta \rho \omega^2 R\, d_h^2}{\sigma}, \quad (5)$$

and a, b, and c are constants that are obtained by comparing Eq. 4 with the experimental data. Equation 4 is one of the many dimensionless correlations that can be derived. For example, instead of the stationary-phase density, it is also possible to use the mobile phase density in the Weber number. Another possibility is to add the stationary- or mobile-phase viscosity to the list of relevant parameters. However, Eq. 4 proved to give an adequate result. The droplet–jet transition did not occur at exactly the same flow rate in each of the three visible channels. The difference in flow rate at which the transition in the first channel and the last channel (of the three channels visible in the mirror) occurred is 0.1–0.4 mL/min. The parameters a, b, and c were obtained by comparing the droplet–jet transition data given in Table 3 with Eq. 4. In this way the following set of parameters was obtained:

$$a = 1.21$$
$$b = -1.38$$
$$c = 1.81.$$

The parameters are valid within the range of the properties of the two-phase system given in Table 1 and Table 2. A parity plot with all the measured and predicted critical flow rates is given in Figure 8. The average deviation between the calculated and the measured critical flow rate is 11%.

Table 3. Measured Channel Entrance Velocities at Which the Droplet–Jet Transition Occurs for a Given Rotational Frequency and for Various Two-Phase Systems

Two-Phase System	$\omega^2 R$ (rad^{2}m/s^2)	v_{crit} (m/s)	Two-Phase System	$\omega^2 R$ (rad^{2}m/s^2)	v_{crit} (m/s)	Two-Phase System	$\omega^2 R$ (rad^{2}m/s^2)	v_{crit} (m/s)
Hexane/water	171	0.128	Octanol/water	199	0.037	HMW 37.5	259	0.072
	293	0.111		218	0.035		422	0.057
	405	0.083		226	0.030		568	0.041
	526	0.080		381	0.024		742	0.033
	578	0.078		486	0.022		994	0.028
	721	0.057		561	0.019	HMW 25	193	0.052
	1051	0.052		717	0.017		297	0.041
	1162	0.050		886	0.013		422	0.030
	1442	0.037	Ethyl acetate/water	124	0.061		572	0.023
	2143	0.026		236	0.033		804	0.017
	3054	0.022		404	0.028		1003	0.011
Heptane/water	273	0.120		524	0.024	HMW 12.5	164	0.035
	474	0.074		618	0.022		261	0.026
	714	0.057		825	0.019		379	0.022
	1173	0.041		1192	0.013		572	0.013
	1978	0.024	Chloroform/water	484	0.057		742	0.011
n-Butanol/water	30	0.026		627	0.048			
	118	0.010		804	0.035			
				1003	0.028			
				1224	0.024			

Conclusions

The different flow regimes that occur in the channels of a CPC column are shown as a function of the flow rate, the rotational frequency, and the properties of several two-phase systems. Two dominant flow regimes are present: the droplet and the (broken) jet regime. The droplet regime is present at low flow rates and rotational frequencies. The number of droplets in a channel increases with increasing flow rate, while the size of the droplets decreases with increasing rotational frequency. A dimensionless correlation is presented that predicts the critical velocity at which the droplet–jet transition occurs. The interfacial tension and the density difference have the largest influence on the droplet size and the critical velocity. The jet regime has many appearances; the jet can be continuous, flowing along the wall, or breaking up in droplets. Increasing the flow rate and the centrifugal acceleration causes the jet to break up. The limited size of the channels makes it difficult to predict how exactly the jet flows through the channels. The just-presented quantitative and qualitative knowledge of the type of flow regimes in a CPC channel is a valuable tool to explain separation efficiency, pressure drop, and stationary-phase holdup as a function of the various parameters. Furthermore, it will be used for the design of improved CPC equipment.

Acknowledgments

The technicians of the Kluyver Laboratory of the Delft University of Technology are thanked for constructing the rotor and the transparent cartridge. The Department of Physical Chemistry of the Delft University of Technology is thanked for providing the tensiometer.

Notation

ω = rotational frequency, rad/s

Literature Cited

Armstrong, D. W., G. L. Bertrand, and A. Berthod, "Study of the Origin and Mechanism of Band Broadening and Pressure Drop in Centrifugal Partition Chromatography," *Anal. Chem.*, **60**, 2513 (1988).

Clift, R., J. R. Grace, and M. E. Weber, *Bubbles, Drops and Particles*, Academic Press, New York (1978).

Conway, W. D., *Countercurrent Chromatography: Apparatus, Theory and Application*, VCH Publishers (1989).

Foucault, A. P., O. Bousquet, and F. Le Goffic, "Importance of the Parameter Vm/Vc in Countercurrent Chromatography: Tentative Comparison Between Instruments Designs," *J. Liq. Chromatog.*, **15**, 2691 (1992).

Foucault, A. P., E. Camacho Frias, C. G. Bordier, and F. Le Goffic, "Centrifugal Partition Chromatography: Stability of Various Biphasicic Systems and Pertinence of the Stokes' Model to Describe the Influence of the Centrifugal Field Upon the Efficiency," *J. Liq. Chromatog.*, **17**, 1 (1994).

Foucault, A. P., "CPC Instrumentation," *Handbook of Centrifugal Partition Chromatography*, A. P. Foucault, ed., Dekker, New York, p. 355 (1995).

Jufu, F., L. Buqiang, and W. Zihao, "Estimation of Fluid-Fluid Interfacial Tensions of Multicomponent Mixtures," *Chem. Eng. Sci.*, **41**, 2673 (1986).

Sørensen, J. M., and W. Arlt, *Liquid-Liquid Equilibrium Data Collection. Binary Systems*, Chemistry Data Ser., Vol. V, Part 1, Dechema, Frankfurt/Main, Germany (1980).

Teja, A. S., and P. Rice, "Generalized Corresponding State Method for the Viscosities of Liquid Mixtures," *Ind. Eng. Chem. Fundam.*, **20**, 77 (1981).

Thornton, J. J., *Science and Practice of Liquid-Liquid Extraction*, Oxford Univ. Press, New York (1992).

Van Buel, M. J., L. A. M. van der Wielen, and K. Ch. A. M. Luyben, "Pressure Drop in Centrifugal Partition Chromatography," *Handbook of Centrifugal Partition Chromatography*, A. P. Foucault, ed., Dekker, New York, p. 51 (1995).

Weast, R. C., *CRC Handbook of Chemistry and Physics*, 60th ed., CRC Press, Boca Raton, FL (1980).

Manuscript received Mar. 10, 1997, and revision received Feb. 2, 1998.